THE EFFICACY OF BAND WEIGHTING SCHEMES FOR IMPROVING THE ACCURACY AND PRECISION OF WATER QUALITY PARAMETERS ESTIMATED FROM MERIS AND MODIS IMAGE DATA

Glenn Campbell[1,2] and Stuart Phinn[1]

[1]Centre for Remote Sensing and Spatial Information Science
University of Queensland, St Lucia QLD 4072

[2]Australian Centre for Sustainable Catchments & Faculty of Engineering and Surveying
University of Southern Queensland, Toowoomba QLD 4350
Phone:+61 7 4631 2909 Facsimile:+61 7 4631 2526
Email: campbelg@usq.edu.au

Abstract

Optical remote sensing has been used to map and monitor water quality parameters such as the concentrations of hydrosols (chlorophyll and other pigments, total suspended material, and coloured dissolved organic matter). One approach to estimate hydrosol concentrations is to apply a Matrix Inversion Method (MIM) to the reflectance in each band, creating a system of linear equations, and then apply a least squares method to solve for the hydrosol concentrations.

The accuracy and precision of this method depends on the width, position and inherent noise in the spectral bands of the sensor being employed, as well as the radiometric corrections applied to images to calculate the subsurface reflectance. It has been suggested that by differentially weighting the band equations in over-determined systems the reliance of the solution on any one band can adjusted. The aim of this work was to establish if this is true and if so, determine the optimal weighting regime for each sensor.

The *Hydrolight®* radiative transfer model and typical hydrosol concentrations from Wivenhoe Dam, a large freshwater storage in South East Queensland, were used to simulate 1089 reflectance spectra for MERIS and MODIS images acquired at two sun positions. The accuracy and precision of hydrosol concentrations derived from each weighting regime were evaluated after errors associated with the air-water interface correction, atmospheric correction and the IOP measurement were modelled and applied to the simulated reflectance spectra. The technique showed the ability of a weighting regime to alleviate the effect of these errors and was used as a measure of a regime's efficacy.

The results of this study will be used to improve an algorithm for the remote sensing of water quality for freshwater impoundments.

Introduction

Optical remote sensing has been used to retrieve water quality parameters such as the concentrations of hydrosols (chlorophyll and other pigments, total suspended material, and coloured dissolved organic matter) to model dynamic environmental processes.

The subsurface reflectance spectrum ($R(\lambda,0^-)$) is a result of the cumulative interactions of light with the water itself and the hydrosols. To retrieve the hydrosol concentrations it is necessary to invert the reflectance spectrum. The hydrosol concentrations and the reflectance spectrum are linked by the inherent optical properties (IOPs) of the water. These three properties have magnitudes that are independent of the geometric structure of the light field. The absorption coefficient *(a)* describes the chances of a photon being absorbed, the scattering coefficient *(b)* describes the chances of a photon being scattered and the volume scattering function (VSF) $(\beta(\theta))$ describes the probability of a scattered photon being scattered in a particular direction. The last two properties are usually combined into the total backscattering probability (b_b) which describes the chances of a photon being scattered in a direction greater than 90° to its initial direction of travel. Any successful semi-analytic inversion approach needs to relate the reflectance to the IOPs and then the IOPs to the hydrosol concentrations.

Each natural water body, via the water IOPs, has distinctive relationships between hydrosol concentrations and the remotely sensed reflectance. This relationship can be linearised and the concentrations can be received from the measured reflectance using the Matrix Inversion Method (MIM). The performance of the method depends on the width, position and inherent noise of the bands of the sensor being employed as well as the corrections applied to images to calculate the subsurface reflectance. Researchers have generally used exactly determined systems of equations of *a priori* selected bands. However it is possible to retain all the information but adjust the reliance of the solution on any one band by using over-determined systems of equations introducing differential weights for each band.

This paper uses the average retrieval error and its 95% confidence interval as a measure of the efficacy of band weighting schemes. It investigates how these measures are affected by uncertainty in the measured spectrum and the model parameters. It also investigates the potential reliable measurement ranges of two satellite sensors most suited to monitoring water quality on a regular basis, MERIS and MODIS. The utility of both sensors to retrieve hydrosol concentrations for Wivenhoe Dam, a large freshwater storage in South East Queensland was assessed.

Study Site and Field Measurements

Lake Wivenhoe is located in the upper Brisbane River in South East Queensland. Risk assessments characterise the overall water quality rating as moderate and the cyanobacterial rating as poor (Orr and Schneider 2006).

During July 2007 the IOPs of the storage were measured at nine stations between the dam wall and the Esk offtake tower. Water samples were taken

from the near surface water and kept cool for later laboratory measurement of total suspended material (TSM), chlorophyll *a* (CHL) concentration and CDOM concentration. The spectral absorption of the hydrosols was measured with a UV /VIS dual beam spectrophotometer with integrating sphere. At each station the water was pumped for a minimum of ten minutes from approximately 0.5m below the surface, settled to remove air bubbles and then gravity fed successively through a conductivity-temperature sensor and a *WET Labs* absorption and attenuation meter (ac-9) (WET Labs 2005) and finally emptied into a black plastic container. In the container the scattering properties were measured using a HydroScat-6 (Maffione and Dana 1997). A separate measurement of the backscattering of phytoplankton cells was not feasible, the assumption was made that 1 µg l^{-1} of CHL was approximately equal to 0.07 mgl^{-1} TSM (Phinn et al., 2005).

Spectra Simulation

The subsurface reflectance was modelled with *Hydrolight 4.2*, a numerical model which solves the radiative transfer equation to produce radiance distributions and derived quantities for natural waters (Mobley and Sundman 2001).

Based on monitoring data over the last 5 years supplied by SEQWater 1089 *Hydrolight®* simulations were run at the hydrosol concentration values shown in Table 1. As SEQWater does not regularly measure CDOM values the range was estimated based on field measurements. Freshwater absorption (Pope and Fry 1997; Smith and Baker 1981) and backscattering (Smith and Baker 1981) were taken from literature.

Table 1 Hydrosol concentrations used in simulation of the reflectance spectra

Hydrosol	Concentration
Chlorophyll *a* (µg l^{-1})	0,2,4,6,8,10,12,14,16,18,20
TSM (mg l^{-1})	0,2,4,6,8,10,12,14,16,18,20
CDOM (a_{CDOM} @440 nm [m^{-1}])	0,0.1,0.2,0.3,0.4,0.5,0.6,0.7,0.8

The simulations were run using average IOP values from the 2007 site visit at 1nm steps between 401-799nm using a clear sky with the default *Hydrolight®* atmosphere, an infinite depth and a windspeed of 1m/s. Two simulations were performed with sun positions at time of MERIS overpass for Wivenhoe for the start of July (Zenith angle = 61.1°) and the time of MODIS overpass for the start of January (Zenith angle = 19.1°). The simulated spectra were then convolved with the MERIS (bands 1-12) and MODIS bands (bands1,3,4, 8-15).

Bio-Optical Model

The subsurface reflectance $R(0^-)$ is related to the absorption and backscattering by the model proposed by Gordon et al.(1975):

$$R(\lambda,0^-) = f(\lambda)\frac{b_b(\lambda)}{a(\lambda)+b_b(\lambda)} \qquad (1)$$

The proportionality factor f is often referred to as the anisotropy factor as it represents a correction for the direction distribution of light in the upwelling and downwelling fields.

From the result of the *Hydrolight®* simulations a quadratic equation for *f* in terms of $R(0^-)$ was calculated (Brando and Dekker 2003) for each sun position. The average error between the fitted curve and the raw data was 1%.

A four part absorption model was used.

$$a(\lambda) = a_w(\lambda) + a_{CDOM}(\lambda) + a_{TSM}(\lambda) + a_\phi(\lambda) \quad (2)$$

The values for $a_w(\lambda)$ were obtained from Pope and Fry (1997). The absorption due to CDOM, TSM and Chlorophyll a_φ is proportional to the concentration of the constituent. This is normally represented by the use of a specific absorption coefficient (a^*)

$$a_i(\lambda) = C_i a_i^*(\lambda). \quad (3)$$

The specific spectra were sourced from averaging the spectra obtained from the field measurements described earlier in the text.

A three part backscattering model was used.

$$b_b(\lambda) = b_{bw}(\lambda) + b_{bTSM}(\lambda) + b_{b\phi}(\lambda). \quad (4)$$

The scattering coefficient for pure water will be obtained from Morel (1974) and a ratio of b_w:b_{bw} of 0.5 will be used. The backscattering of TSM and phytoplankton were obtained from averaging the measured field samples and calculating the specific coefficients as before.

Matrix Inversion Method

The matrix inversion (MIM) approach models the measured reflectance as a function of the absorption and backscattering coefficients in each band and then solves the resultant system of linear equations. With the increase in the number of bands in more recent instruments there have been moves from using exact (same number of bands as unknowns) systems (Brando and Dekker 2003; Hoge and Lyon 1996; Hoge et al., 1999; Hoogenboom et al., 1998; Lyon and Hoge 2006) to over-determined (more bands than unknowns) systems (Boss and Roesler 2006; Hakvoort et al., 2002; Vos et al., 2003).

To recover the hydrosol concentrations Equation 1 is rearranged as a system of N (N = number of bands) linear equations in the form *Ax=y,* with

$$A_{ij} = a_j^*(\lambda_i)\frac{R(\lambda_i)}{f} - b_{bj}^*(\lambda_i)\left(1 - \frac{R(\lambda_i)}{f}\right), \quad \text{i} = 1 \text{ to N and j} = \phi, \text{TSM}, \text{CDOM}$$

$$y_i = a_{wi}(\lambda_i)\frac{R(\lambda_i)}{f} - b_{bwi}(\lambda_i)\left(1 - \frac{R(\lambda_i)}{f}\right) \quad (5)$$

$$x_j = C_j$$

Once the system is over-determined the solution of the equation system cannot be exact because of errors in the measurement and model so the MIM method

uses a measure of consistency and then finds the solution that minimises this error. It has been asserted but not demonstrated that application of the weighted least-squares method significantly improves the accuracy of the results (Hakvoort et al., 2002). There has been little work done on the effects of over-determined systems except a finding that the MIM method was less accurate when using 15 or more bands (Vos et al., 2003) and that the need to convolve the IOPs with the response function of the sensor leads to a biased error especially for broad bands (Keller 2001).

Weighting Schemes

The weight matrix is a square diagonal matrix (W) where W_{ii}= relative weight of band *i*. The weights are chosen to give greater influence to those bands which are deemed to be more reliable. The weighting schemes shown in tables 2-3 are labelled by family group.

The first family of weighting schemes represent the conventional approach where all bands are given equal weighting (ALL & NO_IR) or where exactly determined systems of equations of *a priori* selected bands have been used (3BANDS). In this case the three bands selected were as close as possible to those used by Phinn et al. (2005), two centred at 490 and 670 nm and one in the 700-740 nm range.

The next family of weighting schemes assumes that there is a uniform noise in reflectance (Hakvoort et al., 2002) meaning that those bands with a high value of reflectance should have a higher signal to noise ratio and thus will be more reliable (HAK & REF). As the shape of the reflectance spectrum changes with the concentrations of the hydrosol weights representing low, mid and high hydrosol concentrations were selected.

Giardino et al.(2007) make the argument that bands that exhibit the greatest change in reflectance when an increase in a hydrosol concentration occurs should be of greater use in determining the concentration. The change in reflectance with a change in a hydrosol concentration is measured by the first derivative of the spectra with respect to the hydrosol concentration (DER). Using the *Hydrolight* simulations the derivatives were calculated and used to create the next family of weighting schemes.

The last family were derived empirically (RAN). The weights were allowed to vary randomly and those that performed the best were retained and the commonalities of the best performed schemes were combined.

Modelling Uncertainty

The bio-optical model shown in Equation 1 relates the subsurface reflectance to the absorption and backscattering of the water and hydrosols. As a remote sensor measures the top of atmosphere radiance obtained the effect of the atmosphere and the air-water interface must be eliminated before the subsurface reflectance spectra can be used. In addition the MIM relies on having accurate specific absorption and backscattering spectra. Any measurement errors, approximations or assumptions made in this process will introduce error into the retrieved hydrosol concentrations. The ability of a

weighting scheme to alleviate the effect of these errors will be a useful measure of its efficacy.

To simulate the effect of three broad types of error the following distortions were made to the simulated spectra or the SIOPs:

Environmental noise errors

Some errors act separately in each band meaning the reflectance spectra is distorted in shape as well as scale. Some of the sources of this variation are:

- A single value of the ratio of upwelling irradiance to upwelling radiance (Q) is used in the air-water interface correction of De Haan & Kokke (1996) but the Hydrolight simulations show this value varies by approximately 4%.
- The average error between the fitted curve and the raw data for the anisotropy factor f was 1%.
- The environmental noise-equivalent radiance difference ($NE\Delta R(0^-)_E$) (Brando and Dekker 2003) is the standard deviation of the subsurface reflectance in each band over a homogeneous area of optically deep water. Using a MERIS full resolution acquired on the 2nd July 2007 corrected using c-WOMBAT-c (Phinn et al., 2005) $NE\Delta R(0^-)_E$ was estimated to be a constant 0.1% in all bands.

For eight noise levels between 0-7% these errors were imitated by adding to each band in a simulated spectrum a normally-distributed, pseudo-random number with a mean of zero and a standard deviation of one that was scaled to the particular noise level. An offset representing the $NE\Delta R(0^-)_E$ was then applied. As each band had a different scale factor applied to it the effect was to distort the shape as well as the scale of the spectra. The inversion algorithm was applied and the mean of the 100 mean errors was calculated for each hydrosol value at each noise level.

Atmospheric correction errors

The errors associated with the atmospheric correction involve a scale error and a shape error as before but in this case amount of the error will be band dependent. In broad terms the scale error will occur when an incorrect estimate has been made of the visibility and the shape error will occur from making a poor estimation of the aerosol types or their mixing ratio. The spectral dependence of the path radiance conforms to a power law so the spectra were modified by single scale variable (0-20%, normally distributed) as well as a value for the slope (0-10%) The inversion was run on the 1089 simulated spectra with 100 applications of the noise. The mean of the 100 mean errors was calculated for each hydrosol value at each noise level.

SIOP measurement errors

The MIM method requires that the spectra for a^* and b^*_b be calculated from field measurement of the total absorption and backscattering for each constituent and the hydrosol concentration. Obviously measurement errors in the hydrosol concentration will result in a consistent scale error across all bands. In addition

the measurement of absorption and backscattering for each constituent will have a shape error associated with it. For the phytoplankton absorption the shape change was modelled in the same way as the signal shape error while the other hydrosols' absorption and the backscattering were modelled using a variation of spectral slope in the same way as the atmospheric correction error. After considering the variation in SIOPs measured during the July 2007 site visit the phytoplankton SIOPs the scale error was applied between 0% and 20% and the noise applied to the slope was set at half the value for the scale. The absorption and scattering of pure water was not varied.The inversion was run as described in the previous section.

Results

Baseline Accuracy and Precision Values

To establish the baseline accuracy and precision of the MIM method the *Hydrolight* simulations were inverted and the absolute error was calculated using the simulated concentration as the true value. The error here represents the approximations made in the inversion model and the effect of convolving the raw signal into the sensor bands. Weighting regimes that improve on the performance of the standard three band method are highlighted.

There is a marked difference in the performance of the three band scheme between the two satellite simulations, most probably because MODIS does not have a band strictly within the 700-740nm range.

Table 2 Baseline Accuracy and Precision Values for MERIS- Weighting regimes that improve on the performance of the standard three band method are highlighted in green.

Weighting Scheme	Average error					
	Chlorophyll *a* (µg l^{-1})		TSM (mg l^{-1})		CDOM ([m^{-1}])	
	Jan	Jul	Jan	Jul	Jan	Jul
MER_3BANDS	1.21 ± 0.04	1.36 ± 0.04	0.27 ± 0.01	0.21 ± 0.01	0.31 ± 0.01	0.34 ± 0.01
MER_ALL	4.96 ± 0.14	5.41 ± 0.16	0.35 ± 0.02	0.53 ± 0.02	0.22 ± 0.01	0.25 ± 0.01
MER_HAK	1.90 ± 0.08	2.35 ± 0.09	0.08 ± 0.00	0.08 ± 0.00	0.27 ± 0.01	0.31 ± 0.01
MER_NO_IR	0.94 ± 0.03	0.82 ± 0.03	0.66 ± 0.03	0.56 ± 0.03	0.22 ± 0.01	0.25 ± 0.01
MER_DER1	0.97 ± 0.04	1.45 ± 0.06	0.23 ± 0.01	0.10 ± 0.00	0.25 ± 0.01	0.28 ± 0.01
MER_DER2	1.28 ± 0.06	1.79 ± 0.08	0.11 ± 0.00	0.07 ± 0.00	0.25 ± 0.01	0.28 ± 0.01
MER_DER3	2.11 ± 0.09	2.30 ± 0.08	0.05 ± 0.00	0.11 ± 0.01	0.27 ± 0.01	0.31 ± 0.01
MER_DER4	5.01 ± 0.19	4.81 ± 0.18	2.54 ± 0.13	2.39 ± 0.12	0.15 ± 0.01	0.18 ± 0.01
MER_RAN1	0.18 ± 0.01	0.25 ± 0.01	0.57 ± 0.03	0.49 ± 0.03	0.24 ± 0.01	0.27 ± 0.01
MER_RAN2	0.41 ± 0.01	0.43 ± 0.02	0.48 ± 0.02	0.40 ± 0.02	0.24 ± 0.01	0.27 ± 0.01
MER_RAN3	0.50 ± 0.02	0.57 ± 0.02	0.34 ± 0.02	0.27 ± 0.02	0.24 ± 0.01	0.27 ± 0.01
MER_RAN4	1.45 ± 0.06	1.76 ± 0.07	0.14 ± 0.01	0.06 ± 0.00	0.23 ± 0.01	0.26 ± 0.01
MER_RAN5	2.12 ± 0.07	2.57 ± 0.10	0.22 ± 0.01	0.11 ± 0.01	0.21 ± 0.01	0.24 ± 0.01
MER_RAN6	4.95 ± 0.14	5.52 ± 0.17	0.42 ± 0.02	0.61 ± 0.03	0.32 ± 0.01	0.35 ± 0.01
MER_RAN7	9.07 ± 0.22	9.41 ± 0.25	0.35 ± 0.02	0.50 ± 0.03	0.14 ± 0.01	0.17 ± 0.01
MER_RAN8	14.3 ± 0.38	14.6 ± 0.40	0.20 ± 0.01	0.30 ± 0.02	0.05 ± 0.00	0.09 ± 0.00
MER_REF1	1.43 ± 0.04	1.05 ± 0.05	0.56 ± 0.03	0.41 ± 0.02	0.28 ± 0.01	0.31 ± 0.01
MER_REF2	1.46 ± 0.07	1.95 ± 0.08	0.15 ± 0.01	0.05 ± 0.00	0.27 ± 0.01	0.30 ± 0.01

Table 3 Baseline Accuracy and Precision Values for MODIS- Weighting regimes that improve on the performance of the standard three band method are highlighted in green.

Weighting Scheme	Average error					
	Chlorophyll *a* (µg l^{-1})		TSM (mg l^{-1})		CDOM ([m^{-1}])	
	Jan	Jul	Jan	Jul	Jan	Jul
MOD_3BANDS	12.1 ± 0.08	12.5± 0.10	1.57 ± 0.06	1.75 ± 0.07	0.29 ± 0.01	0.32 ± 0.01
MOD_ALL	3.28 ± 0.12	3.75 ± 0.14	0.52 ± 0.02	0.70 ± 0.03	0.24 ± 0.01	0.28 ± 0.01
MOD_HAK	1.40 ± 0.04	1.16 ± 0.05	0.38 ± 0.02	0.24 ± 0.01	0.30 ± 0.01	0.33 ± 0.01
MOD_NO_IR	7.96 ± 0.27	7.87 ± 0.26	2.01 ± 0.11	1.92 ± 0.11	0.20 ± 0.01	0.23 ± 0.01
MOD_DER1	3.79 ± 0.09	3.49 ± 0.07	0.87 ± 0.05	0.73 ± 0.04	0.26 ± 0.01	0.29 ± 0.01
MOD_DER2	6.94 ± 0.25	6.95 ± 0.24	3.10 ± 0.15	2.97 ± 0.15	0.13 ± 0.01	0.15 ± 0.01
MOD_DER3	2.81 ± 0.06	2.49 ± 0.05	0.70 ± 0.04	0.56 ± 0.03	0.27 ± 0.01	0.30 ± 0.01
MOD_DER4	0.85 ± 0.03	1.11 ± 0.04	0.26 ± 0.01	0.12 ± 0.00	0.29 ± 0.01	0.32 ± 0.01
MOD_RAN1	0.57 ± 0.02	0.96 ± 0.04	0.33 ± 0.02	0.20 ± 0.01	0.20 ± 0.01	0.23 ± 0.01
MOD_RAN2	2.08 ± 0.09	2.61 ± 0.11	0.15 ± 0.01	0.34 ± 0.01	0.18 ± 0.01	0.22 ± 0.01
MOD_RAN3	0.59 ± 0.03	0.80 ± 0.03	0.45 ± 0.02	0.31 ± 0.01	0.17 ± 0.01	0.21 ± 0.01
MOD_RAN4	11.5 ± 0.25	11.8 ± 0.27	1.07 ± 0.05	1.25 ± 0.06	0.13 ± 0.01	0.17 ± 0.01
MOD_RAN5	0.56 ± 0.02	0.95 ± 0.04	0.33 ± 0.02	0.20 ± 0.01	0.20 ± 0.01	0.23 ± 0.01
MOD_RAN6	0.76 ± 0.04	0.76 ± 0.03	0.71 ± 0.04	0.62 ± 0.03	0.18 ± 0.01	0.21 ± 0.01
MOD_REF1	2.23 ± 0.05	1.89 ± 0.05	0.56 ± 0.03	0.42 ± 0.02	0.28 ± 0.01	0.31 ± 0.01

Accuracy and Precision Values after the Addition of Environmental Noise

Before introducing simulated error form the other sources the offset representing the $NE\Delta R(0^-)_E$ was applied. Figure 1 shows the average error before the application of the noise plotted against the average error after the noise is applied. The highlighted data points are for the standard three band method.

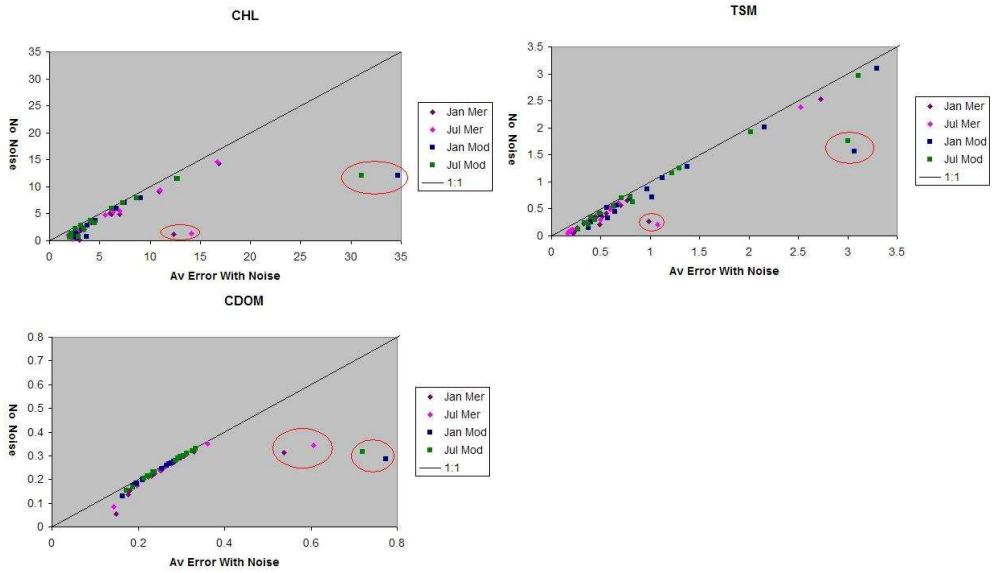

Figure 1 Plot of Average Error response to the application of $NE\Delta R(0^-)_E$ error

While the other weighting schemes show a reasonably linear trend the three band method shows is shown to respond very poorly to the introduction of the $NE\Delta R(0^-)_E$ error.

As the level of noise is increased the majority of weighting schemes exhibit an exponential increase in the average error for chlorophyll *a* and TSM values for both MERIS and MODIS. The schemes where all bands were given equal weighting were unaffected by the increase in noise but their performance was still inferior even at high noise levels. The CDOM average error is virtually unaffected by the increase in noise for most weighting schemes with some (MOD_HAK & MOD_DER) slightly improving. However their performance was still inferior to other schemes even at high noise levels.

Accuracy and Precision Values after the Addition of Atmospheric Noise

As before the CDOM average error was shown to be practically unaffected by the introduced noise but there was a linear increase in the confidence level of the average. In all but one case the TSM accuracy and precision exhibited a linear increase with an increase of atmospheric noise. The slope of this trend line varied very little between the weighting schemes. There was however significant variation in the performance with respect to chlorophyll *a* retrieval error. The MER_HAK and MER_DER1 weighting schemes were similar but the performance of the MER_HAK was insensitive to the presence of the atmospheric error. (Figure 2) Both schemes are similar except for the weight given to band 9. To see if this greater weight in band 9 controlled the response MER_DER1 was changed to have a greater weight in band 9 (MER_DER5). As a result the effect of the noise was reduced by a significant (at 95%) amount. This behaviour is also displayed by the best overall performer MER_RAN3 which has a strong weight on band 9. The best performer at low noise MER_RAN1 performed more poorly as the noise increased. Increasing the weight of band 9 improved its insensitivity but at the cost of a worse performance at lower noise levels.

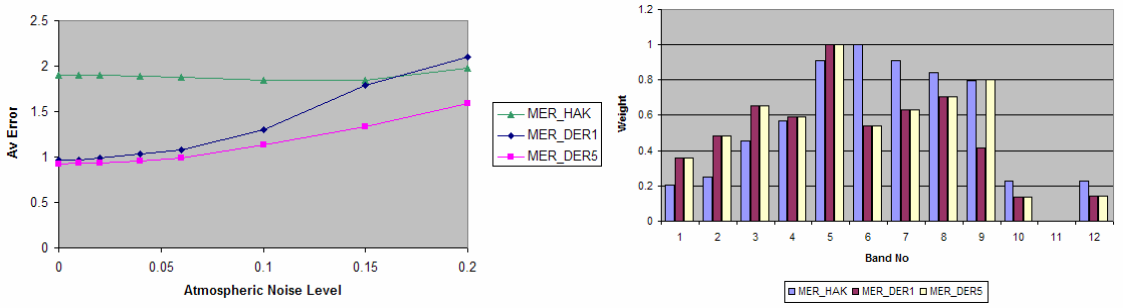

Figure 2 Plot of the average error of Chlorophyll *a* retrieval against the atmospheric noise level (L) and a plot of the respective weighting schemes (R)

Accuracy and Precision Values after the Addition of SIOP Noise

The plot of the CDOM average error appears to be bilinear. The average error is practically unaffected by the introduced noise until the noise reaches

approximately 8% then there is a linear increase with increased noise. This effect is more pronounced with the MERIS simulation. As with the atmospheric noise the TSM accuracy and precision exhibited a linear increase with an increase of atmospheric noise. The slope of this trend line varied very little between the weighting schemes. In the MERIS simulation for the low levels of SIOP noise only four weighting schemes perform better than three band option for chlorophyll *a.* However the three band option's performance deteriorates in the presence of greater SIOP error. Once again there are some schemes that are insensitive to the SIOP error but their performance at lower noise levels means that they are not preferred.

Effect of the anisotropy factor (f)

It was found during the error calculation process that the increased error associated with the sources of noise was dwarfed by the effect of changes to the anisotropy factor. If the calculated quadratic expression was replaced by the approximation that depends only on the sun zenith, $f = \frac{1}{1+2\mu_0}$ (Phinn et al., 2005) the average error for the January MERIS simulation increased from by 20-650% for chlorophyll *a* and 230-2000% for TSM. Paradoxically the average error for CDOM retrieval was reduced by a factor of 2-10.

Conclusions

This paper shows that the use of over-determined systems improves the performance of the hydrosol concentration retrieval in terms of accuracy and precision. Furthermore, differentially weighting the bands in the over-determined systems improves the performance of the hydrosol concentration retrieval in terms of accuracy and precision and in some circumstances the use of differential weighting has mitigated against the effect of noise in the remote sensing system. Howeve,r the simulations show that effort put into better determinations of the anisotropy factor would be more productive.

Acknowledgements

The authors would like to thank Mr Paul Daniels, Dr Arnold Dekker and Dr Vittorio Brando of CSIRO for assistance in the field work and SEQWater for the provision of historical water quality data.

References

BOSS, E. and ROESLER, C. S. (2006). Over Constrained Linear Matrix Inversion with Statistical Selection. *Report of the International Ocean-Colour Coordinating Group No. 5: Remote Sensing of Inherent Optical Properties: Fundamentals, Tests of Algorithms, and Applications* Z. Lee (eds). Dartmouth, Canada, International Ocean-Colour Coordinating Group.

BRANDO, V. E. and DEKKER, A. G. (2003). Satellite hyperspectral remote sensing for estimating estuarine and coastal water quality. *IEEE Transactions on Geoscience and Remote Sensing,* 41, 1378-1387.

DE HAAN, J. F. and KOKKE, J. M. M. (1996). *Remote Sensing Algorithm Development TOOLKIT I: Operationalisation of Tools for Atmospheric Correction of Remote Sensing Data of Coastal and Inland Waters*, Beleidscommissie Remote Sensing.

GIARDINO, C., BRANDO, V. E., DEKKER, A. G., STROMBECK, N. and CANDIANI, G. (2007). Assessment of water quality in Lake Garda (Italy) using Hyperion. *Remote Sensing of Environment,* 109, 183-195.

GORDON, H. R., BROWN, O. B. and JACOBS, M. M. (1975). Computed relationships between the inherent and apparent optical properties of a flat homogeneous ocean. *Applied Optics,* 14, 417-427.

HAKVOORT, H., DE HAAN, J. F., JORDANS, R. R. W., VOS, R. J., PETERS, S. W. M. and RIJKEBOER, M. (2002). Towards airborne remote sensing of water quality in The Netherlands--validation and error analysis. *ISPRS Journal of Photogrammetry and Remote Sensing,* 57, 171-183.

HOGE, F. E. and LYON, P. E. (1996). Satellite retrieval of inherent optical properties by linear matrix inversion of oceanic radiance models: An analysis of model and radiance measurement errors. *Journal of Geophysical Research,* 101, 16631-16648.

HOGE, F. E., WRIGHT, C. W., LYON, P. E., SWIFT, R. N. and YUNGEL, J. K. (1999). Satellite Retrieval of the Absorption Coefficient of Phytoplankton Phycoerythrin Pigment: Theory and Feasibility Status. *Applied Optics,* 38, 7431-7441.

HOOGENBOOM, H. J., DEKKER, A. G. and DE HAAN, J. F. (1998). Retrieval of Chlorophyll and Suspended Matter from Imaging Spectrometry Data by Matrix Inversion. *Canadian Journal of Remote Sensing,* 24, 144-152.

KELLER, P. A. (2001). Comparison of two inversion techniques of a semi-analytical model for the determination of lake water constituents using imaging spectrometry data. *The Science of The Total Environment,* 268, 189-196.

LYON, P. E. and HOGE, F. E. (2006). The Linear Matrix Inversion Algorithm. *Report of the International Ocean-Colour Coordinating Group No. 5: Remote Sensing of Inherent Optical Properties: Fundamentals, Tests of Algorithms, and Applications* Z. Lee (eds). Dartmouth, Canada, International Ocean-Colour Coordinating Group.

MAFFIONE, R. A. and DANA, D. R. (1997). Instruments and methods for measuring the backward-scattering coefficient of ocean waters. *Applied Optics,* 36, 6057-6067.

MOBLEY, C. D. and SUNDMAN, L. (2001). *Hydrolight 4.2 Users' Guide.* Redmond, WA, Sequoia Scientific, Inc.

MOREL, A. (1974). Optical properties of pure water and pure seawater. *Optical aspects of oceanography*. N. G. Jerlovet al (eds), Academic. 1-24.

ORR, P. T. and SCHNEIDER, P. M. (2006). *Toxic Cyanobacteria Risk Assessment: Reservoir Vulnerability and Water Use Best Practice*. Brisbane, SEQ Water**:** 74.

PHINN, S. R., ROELFSEMA, C., SCARTH, P., DEKKER, A. G., BRANDO, V. E., ANSTEE, J. M. and MARKS, A. (2005). *An integrated remote sensing approach for adaptive management of complex coastal waters. Final*

Report - Moreton Bay Remote Sensing Tasks (MR2), CRC for Coastal Zone, Estuary & Waterway Management. Estuary & Waterway Management, Indooroopilly., CRC for Coastal Zone.

POPE, R. M. and FRY, E. S. (1997). Absorption spectrum (380 -700 nm) of pure water. II. Integrating cavity measurements. *Applied Optics,* 36, 8710-8723.

SMITH, R. C. and BAKER, K. S. (1981). Optical properties of the clearest natural waters (200-800 nm). *Applied Optics,* 20, 177-184.

VOS, R. J., HAKVOORT, J. H. M., JORDANS, R. R. W. and IBELINGS, B. W. (2003). Multiplatform optical monitoring of eutrophication in temporally and spatially variable lakes. *The Science of The Total Environment,* 312, 221-243.

WET LABS (2005). *ac-9 Protocol Document, Revision J, 11 April 2005*.